Cell, Vol. 91, 685–694, November 28, 1997, Copyright ©1997 by Cell Press

The MinE Ring: An FtsZ-Independent Cell Structure Required for Selection of the Correct Division Site in E. coli

David M. Raskin and Piet A. J. de Boer*
Department of Molecular Biology and Microbiology
Case Western Reserve University School of Medicine
Cleveland, Ohio 44106-4960

Summary

E. coli cell division is mediated by the FtsZ ring and associated factors. Selection of the correct division site requires the combined action of an inhibitor of FtsZ ring formation (MinCD) and of a topological specificity factor that somehow prevents MinCD action at the middle of the cell (MinE). Here we show that a biologically active MinE-Gfp fusion accumulates in an annular structure near the middle of young cells. Formation of the MinE ring required MinD but was independent of MinC and continued in nondividing cells in which FtsZ function was inhibited. The results indicate that the MinE ring represents a novel cell structure, which allows FtsZ ring formation at midcell by suppressing MinCD activity at this site.

Introduction

Bacteria normally divide at the midpoint of the long axis of the cell (midcell). How the division machinery selects this site over other sites in the cell is not well understood.

Formation of the division septum in Escherichia coli occurs by the circumferential invagination of the cell wall. This process is mediated by the septal ring, a cytoskeletal-like organelle that is associated with the cytoplasmic membrane at the site of division. The septal ring is assembled at the prospective division site well before invagination is initiated and remains associated with the leading edge of the invaginating septum until septal closure (Lutkenhaus and Mukherjee, 1996; Hale and de Boer, 1997; Rothfield and Justice, 1997). Several of the essential division proteins have been shown to be part of the structure (Bi and Lutkenhaus, 1991; Addinall et al., 1996; Addinall and Lutkenhaus, 1996; Ma et al., 1996; Hale and de Boer, 1997). The earliest known step in assembly of the organelle is formation of the FtsZ ring. This annular element is a major component of the septal ring structure and is thought to consist of a homopolymeric form of the key division protein FtsZ. FtsZ is an evolutionary, well-conserved, tubulin-like GTPase that can polymerize in vitro, suggesting that formation of the FtsZ ring in vivo is driven by a self-assembly reaction (de Boer et al., 1992a; RayChaudhuri and Park, 1992; Lutkenhaus, 1993; Mukherjee et al., 1993; Mukherjee and Lutkenhaus, 1994; Baumann and Jackson, 1996; Erickson et al., 1996; Margolin et al., 1996). How this process is initiated at specific sites in the cell is not yet known but conceivably involves the interaction with a hypothetical membrane factor that would mark potential division sites (PDSs) and stimulate polymerization of FtsZ at these sites (Lutkenhaus, 1993). Once the FtsZ ring is formed, other essential division proteins are recruited to form a fully functional septal ring organelle (Addinall et al., 1996; Addinall and Lutkenhaus, 1996).

Whereas the division septum is placed accurately at midcell under normal conditions, this is not the only site where septum formation can occur. Work on minicell mutants (*min*$^-$) has indicated that a PDS is also present at each of the cell poles. In Min$^-$ cells, the frequency of septation is not affected, but the septum is formed at any one of the available PDSs in what appears to be a random fashion. Thus, whereas cells can still divide at midcell, they frequently divide near one of the cell poles instead, resulting in the formation of small, chromosomeless minicells and multinucleate cells that are larger than normal (Adler et al., 1967; Teather et al., 1974; Donachie and Begg, 1996). In wild-type cells, usage of polar PDSs is specifically suppressed by the combined actions of the protein products of the *minB* operon, MinC, MinD, and MinE (de Boer et al., 1988, 1989; Rothfield and Zhao, 1996). MinC is a division inhibitor that, under normal conditions, requires the MinD protein for its activity (de Boer et al., 1990, 1992b). MinD is an ATPase that is peripherally associated with the cytoplasmic membrane (de Boer et al., 1991). Although it is not clear exactly how MinD stimulates MinC function, recent yeast two-hybrid experiments indicate that this process involves a direct interaction between the two proteins (Huang et al., 1996). MinCD activity leads to a block in the assembly of the FtsZ ring (Bi and Lutkenhaus, 1993), and this block can be suppressed by certain *ftsZ* alleles (Bi and Lutkenhaus, 1990) or by overexpression of native FtsZ (Ward and Lutkenhaus, 1985; de Boer et al., 1990). The mechanism by which MinCD prevents formation of the FtsZ ring is not yet known.

MinE is a small protein (88 aa) with at least two functions. The protein not only suppresses MinCD-mediated division inhibition, but also appears to be capable of distinguishing midcell from the cell poles. Thus, in the absence of MinE, MinCD blocks division at all PDSs, leading to the formation of long filamentous cells (Sep$^-$). At normal levels of MinE, however, MinCD activity becomes restricted to the polar PDS. Consequently, division is still blocked at the cell poles but allowed at midcell, giving rise to the normal division pattern. Overexpression of MinE causes suppression of MinCD action at all PDSs in the cell and, therefore, loss of topological specificity. As a result, cells show the classical minicell phenotype (Min$^-$), which is also seen in cells in which MinC and/or MinD is absent (de Boer et al., 1989).

Based on deletion analyses, the two properties of MinE correspond to different domains on the peptide. Whereas the N-terminal 23 aa (αCD domain) of MinE are sufficient to counteract MinCD-mediated division inhibition, the topological specificity of the protein requires, at least, aa 23–81 (TS domain). Thus, MinE derivatives that possess the αCD domain but lack the TS domain (MinE^{TS-}) still suppress MinCD-mediated division inhibition but have lost the ability to restrict this

*To whom correspondence should be addressed.

function to the PDS at midcell. Consequently, coexpression of MinCD with MinE^{TS-} leads to a minicell, rather than a wild-type division phenotype (Pichoff et al., 1995; Zhao et al., 1995).

Two possible strategies by which MinE could impart topological specificity to MinCD action were originally proposed (de Boer et al., 1989), and subsequent genetic studies have been interpreted to support either model. In the first model, MinE itself accumulates at midcell, restricting MinCD-suppressing activity to this site (Zhao et al., 1995; Huang et al., 1996; Rothfield and Zhao, 1996). In the second, MinE accumulates at the cell poles and acts as a pilot peptide to direct MinCD away from midcell (Pichoff et al., 1995).

To distinguish between these possibilities, we have studied the cellular location of biologically active MinE derivatives that were fused to green fluorescent protein (Gfp). The results show that MinE-Gfp accumulates at or near the middle of young cells in a ringlike structure that appears to be associated with the cell envelope. Moreover, several lines of evidence indicate that the MinE ring represents an autonomous cell structure that is formed independently of the septal ring organelle. The MinD protein is shown to play a critical role in assembly of the MinE ring, which is remarkable in light of the fact that MinD is also required to stimulate MinC-mediated division inhibition. Our results support a model in which the MinE ring is instrumental in selection of the proper division site by causing suppression of MinCD activity at midcell, allowing subsequent FtsZ ring and septal ring formation at this site.

Results

Biological Activities of MinE-Gfp Fusion Proteins

To study the cellular distribution of MinE, we used two fluorescent derivatives in which amino acid 88 (MinE-Gfp) or aa 34–88 (MinE*-Gfp), respectively, were substituted with a bright variant (Mut2) of the green fluorescent protein from Aequorea victoria (Cormack et al., 1996). As indicated in Figure 1, two types of plasmid were used to express the fusion proteins in E. coli. The first type contained *minE-gfp* or *minE*-gfp* downstream of the spectinomycin resistance gene (*aadA*) of the pSC101 derivative pZC100, resulting in a moderate level of constitutive expression (de Boer et al., 1990; Zhao et al., 1995). The second type contained the genes downstream of the *lac* promotor of pMLB1115 (de Boer et al., 1989), rendering expression inducible by IPTG (isopropyl β-D-thiogalactoside).

Overexpression of MinE is known to induce a minicell phenotype in wild-type cells (de Boer et al., 1988, 1989), and both MinE-Gfp and MinE*-Gfp retained this property. Thus, in the presence of 250 μM IPTG, both pDR113[P_{lac}::*minE-gfp*] and pDR142[P_{lac}::*minE*-gfp*] caused a minicell phenotype (Min$^-$) in strain PB103 [wt], which was indistinguishable from that caused by pDB156[P_{lac}::*minE*] (data not shown).

To define the biological activities of the fusion proteins further, we made use of strain PB114(λDB173)[Δ*minCDE*(P_{lac}::*minCD*)], which lacks the chromosomal *minB* operon but is lysogenic for a λ derivative expressing the

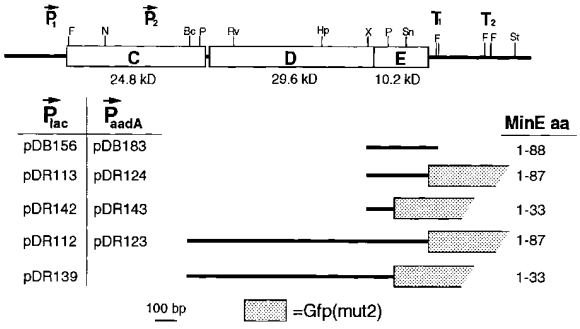

Figure 1. Plasmid Constructs

The physical map of the *minB* operon (de Boer et al., 1989) is shown on top. Indicated are the positions of genes *minC*, *minD*, and *minE*, promotors *P1* and *P2*, probable transcription terminators T1 and T2, and restriction sites for BclI (Bc), FokI (F), HpaI (Hp), NsiI (N), PstI (P), EcoRV (Rv), SnaBI (Sn), StyI (St), and XmnI (X). Inserts of plasmids used in this study are shown below the map. Indicated is whether inserts were present downstream of the *lac* promotor of vector pMLB1115 (P_{lac}) or downstream of the *aadA* gene of vector pZC100 (P_{aadA}). Plasmids pDB156 and pDB183 encode native MinE (88 aa). The other plasmids encode fusion proteins in which residues 1–87 (MinE-Gfp) or 1–33 (MinE*-Gfp) of MinE are joined by peptide EDPPAEF or LEDPPAEF, respectively, to the complete Gfpmut2 protein (Cormack et al., 1996). As indicated, plasmids pDR112, pDR123, and pDR139 expressed native MinD in *cis* with either MinE-Gfp or MinE*-Gfp.

minC and *minD* genes under control of the *lac* promotor (de Boer et al., 1989). As a consequence, this strain is Min$^-$ in the absence of inducer but forms long nonseptate filaments (Sep$^-$) in the presence of IPTG (Figures 2a and 2b). PB114(λDB173) was transformed with the appropriate pZC100 derivatives and examined after growth in the presence of IPTG. Interestingly, like pDB183 [aadA::*minE*] (de Boer et al., 1990; Zhao et al., 1995), pDR124 [aadA::*minE-gfp*] fully restored the normal division pattern (Figures 2c and 2d), showing that MinE-Gfp had not only retained the ability to suppress the MinCD-mediated division block, but also the ability to do this in a topologically specific fashion. Plasmid pDR143 [aadA::*minE*-gfp*] also efficiently suppressed the Sep$^-$ phenotype of PB114 (λDB173). In contrast to pDB183 and pDR124, however, pDR143 failed to restore the wild-type division phenotype but, rather, gave rise to a Min$^-$ phenotype (Figure 2e). This result implied that MinE*-Gfp was still capable of suppressing MinCD-mediated division inhibition but had lost the ability to confer topological specificity to the Min system. Since MinE*-Gfp lacks the carboxy terminal portion of MinE, our results are consistent with the finding that the αCD (suppression of MinCD) and TS (topological specificity) properties of MinE are separable and associated with two different domains in the peptide (Pichoff et al., 1995; Zhao et al., 1995). We conclude that addition of the Gfp moiety did not substantially interfere with the known properties of MinE.

MinE-GFP Is Present in a Centrally Located Ring Structure

As discussed further below, the specific localization of MinE-Gfp was most readily observed in cells in which

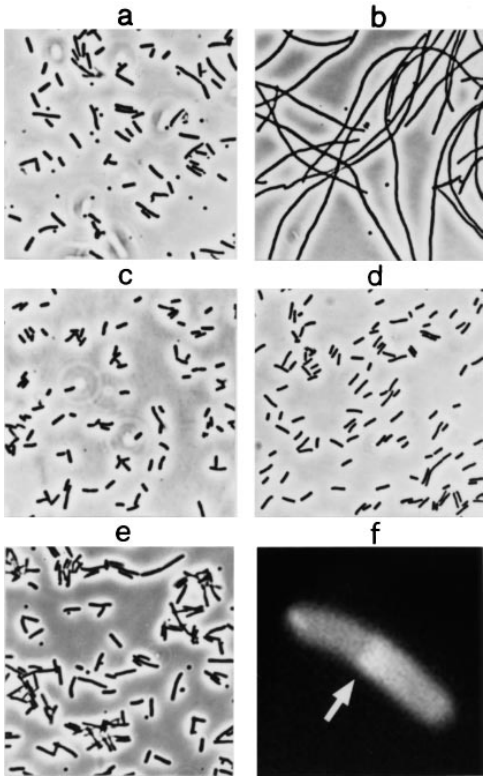

Figure 2. Physiological Properties of MinE-Gfp and MinE*-Gfp

Phase (a–e) and fluorescence (f) micrographs of strain PB114(λDB173) [ΔminCDE(P_{lac}::*minCD*)] carrying plasmid pZC100 (vector) (a and b), pDB183 [aadA::*minE*] (c), pDR124 [aadA::*minE-gfp*] (d and f), or pDR143 [aadA::*minE*-gfp*] (e). (f) shows a typical live PB114(λDB173)/pDR124 cell. Note the centrally located ring structure (arrow), which is partly obscured by a relatively high level of background fluorescence throughout the cell (see also text). Cells were grown in the presence of either 50 μM IPTG (b–f) or 0.1% glucose (a). In the absence of IPTG, cells carrying plasmids pDB183, pDR124, or pDR143 displayed the same Min^- phenotype as is shown in (a).

the fusion was coexpressed with the MinD protein from plasmid constructs in which *minE-gfp* was placed in the "natural" position of *minE*, immediately downstream of the *minD* gene. Figures 3a–3e show cells of wild-type strain PB103 carrying plasmid pDR112 [P_{lac}::*minDE-gfp*] after growth in the presence of 25 μM IPTG. At this low concentration of inducer, cells of PB103/pDR112 showed a wild-type division pattern, with the exception that an occasional polar septum was observed (4 out of 206 cells showed a polar septum). Interestingly, inspection by fluorescence (a–e) and differential interference contrast (a′–e′) microscopy revealed that the majority of MinE-GFP had accumulated at or near the middle of these cells in a ringlike structure that appeared to be associated with the cell envelope. When cells were viewed perpendicular to their long axes, the fluorescent signal appeared as a narrow zone that ran across the width of the cell. The annular shape of this signal, however, was clearly discerned when cells were viewed head on (Figures 3e and 3f) and as they tumbled through the focal plane during examination (not shown).

Based on our observations of live PB103/pDR112 cells immediately upon their application to microscope

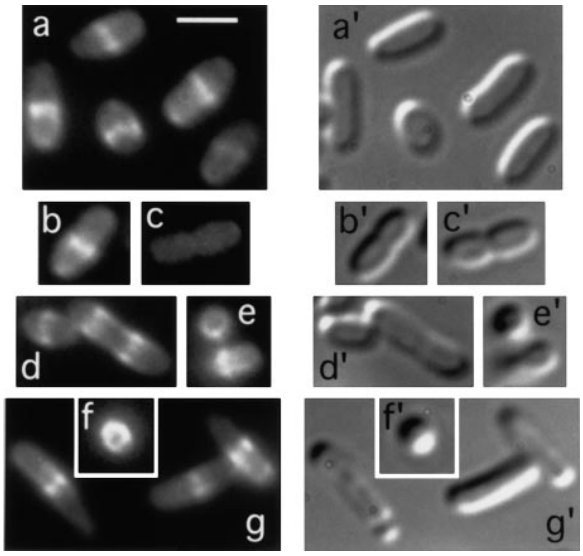

Figure 3. Identification of the MinE Ring

Plasmid pDR112[P_{lac}::*minDE-gfp*] was introduced into strains PB103 [wt] (a–e) and PB114 [Δ*minCDE*] (f and g), and cells were grown in the presence of 25 μM IPTG and fixed before observation by fluorescence (a–g) and DIC (a′–g′) microscopy. The bar represents 2.0 μm.

slides, we estimate that MinE-Gfp rings were present in the vast majority (>80%) of the cell population. A more accurate determination proved difficult to make, since ring structures quickly dissipated as soon as live cells settled down on the glass surface (data not shown). This phenomenon was not alleviated by various pretreatments of the microscope slides, and the reason for this apparent instability of the structure is not clear. Chemical fixation allowed us to obtain faithful images of the MinE ring structures in immobilized cells. Even when using an optimized protocol, however, the procedure still resulted in poorly defined fluorescence signals in about half (48%) the cell population, and this fraction increased rapidly upon storage of the treated cells (data not shown).

In both live and fixed preparations, rings were observed in cells of all sizes, including very small cells (Figures 3 and 4a). This observation indicates that MinE localizes to midcell well before the start of cell constriction and that the ring remains at this site throughout cell elongation. Interestingly, however, clearly defined MinE-GFP ring structures were absent in the majority of cells undergoing constriction. Ring structures were sometimes still present in cells with a shallow constriction (Figure 3b), but the fluorescent signal was diffusely distributed in all deeply constricted cells we observed (Figure 3c). The absence of MinE rings in the latter class of cells suggests that the structure is disassembled during, or shortly after, the initiation of cell constriction.

Almost all cells with a clear localization pattern showed a single ring (>99%) at or near midcell (Figures 3 and 4a). In addition, a few long cells that had likely experienced a delay in septum formation showed two rings at one-fourth and three-fourths of the cell body, respectively (Figure 3d). The presence of such cells indicated that the localization of MinE to future division sites

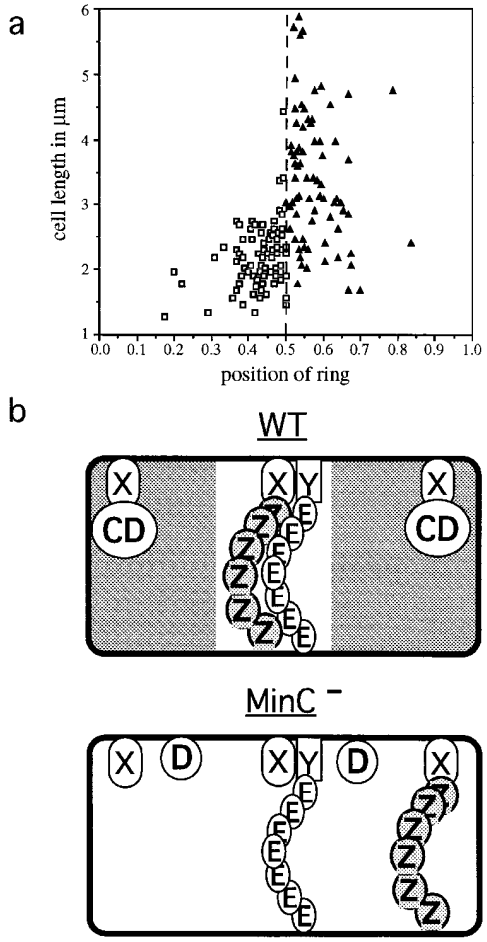

Figure 4. Location of the MinE Ring and Model for MinE Ring Function

(a) Analysis of MinE ring position in wild-type and MinC⁻ cells. Micrographs of 205 and 206 randomly selected cells of strain PB103/pDR112 [wt/P_{lac}::*minDE-gfp*] and PB114/pDR112 [Δ*minCDE*/P_{lac}::*minDE-gfp*], respectively, were obtained as described in the legend to Figure 3. For each cell with a well-preserved single-ring structure (107 and 80 cells, respectively), the cell length, as well as the distance (expressed as a fraction of cell length) of the ring to the most proximal (PB103/pDR112, open squares) or distal (PB114/pDR112, filled triangles) cell pole, was determined. Note that cells with multiple ring structures (see text) were not included in this analysis.

(b) Model for MinE ring function in wild-type cells (WT, top panel). As in previous models (Zhao et al., 1995; Huang et al., 1996), the existence of two hypothetical elements that mark special sites on the cell envelope is assumed. One of these (X) is present at midcell as well as at the cell poles and defines PDSs. The other (Y) acts as the topological target of MinE(E) and uniquely defines the position of the MinE ring at or near midcell. While MinCD (CD) inhibits usage of the polar PDS, MinCD activity (shaded area) is suppressed in proximity of the MinE ring (unshaded area), allowing assembly of the FtsZ ring at the PDS at midcell. In the absence of a functional division inhibitor (MinC⁻, bottom panel), FtsZ/septal ring formation is allowed at any PDS regardless of whether a MinE ring is present at midcell or not. See text for more details.

can occur before septum formation is completed at the old site. Additional results that are consistent with this interpretation are described below.

The accumulation of MinE at or near the middle of normally dividing cells is incompatible with models in which MinE tethers MinCD to the cell poles. On the contrary, our observations provide strong evidence for the proposal that MinE allows the assembly of the division machinery at the nascent division site at midcell by suppressing MinCD action specifically at this site.

MinE Ring Formation Is Independent of the FtsZ Ring

To date, the assembly of the FtsZ ring at the prospective division site is the earliest recognized step in formation of the septal ring organelle (Bi and Lutkenhaus, 1991; Addinall and Lutkenhaus, 1996; Rothfield and Justice, 1997). In addition, MinCD has been shown to inhibit cell division by blocking this step (Bi and Lutkenhaus, 1993). In our model for MinCDE action, therefore, the MinE ring normally allows the FtsZ ring to be assembled at the PDS at midcell. An important prediction of this model is that formation of the MinE ring should be independent of FtsZ ring formation. We tested this prediction by studying the cellular location of MinE-Gfp in cells in which FtsZ ring assembly was prevented.

SfiA is a MinCD-independent division inhibitor that is normally not expressed but induced as part of the SOS response to DNA damage. The protein binds directly to FtsZ and, like MinCD, was shown to block formation of the FtsZ ring (Bi and Lutkenhaus, 1993; Higashitani et al., 1995; Huang et al., 1996). To determine MinE-Gfp localization under conditions of SfiA-mediated filamentation, we constructed strain PB114(λDR144)/pDR123 [ΔminCDE(P_{lac}::sfiA)/aadA::minDE-gfp] in which *sfiA* is placed under control of the *lac* promotor on the lysogenic phage λDR144 and in which MinD and MinE-Gfp are expressed constitutively from plasmid pDR123. As expected, growth of PB114(λDR144)/pDR123 in the presence of IPTG led to the formation of nonseptate filaments (Figures 5a′ and 5b′). Strikingly, inspection by fluorescence microscopy revealed the presence of multiple MinE ring structures located at regular intervals along the length of each of these filaments (Figures 5a and 5b). These results indicated that MinE ring assembly can proceed under conditions where FtsZ ring formation is prevented.

In support of these results, we next studied MinE ring formation in filaments from which the FtsZ protein had been specifically depleted. Because the fluorescent signal of MinE-Gfp diminished significantly at elevated temperatures (data not shown), we constructed strains for this purpose, which allowed for a cold-induced depletion of FtsZ ($FtsZ^{CID}$). One such strain is DR102/pDB346/pDR112 [*ftsZ*^{0}, Δ*minCDE*/$P_{\lambda R}$::*ftsZ*, *cI*857/P_{lac}::*minDE-gfp*], which carries pDR112 [P_{lac}::*minDE-gfp*] to allow for the induction of *minD* and *minE-gfp* as described above. In addition, the strain contains an *ftsZ* null allele in the chromosome (*ftsZ*^{0}), and FtsZ is supplied by plasmid pDB346 [$P_{\lambda R}$::*ftsZ*, *cI857*] in which *ftsZ* transcription is placed under control of the λ*R* promotor and a temperature-sensitive allele of λ repressor. When grown at 42°C, this strain produced short rods and minicells and the FtsZ protein was moderately overexpressed (data not shown). At 30°C, in contrast, cells formed long nonseptate filaments. This is illustrated in Figures 5e′ and 5f′,

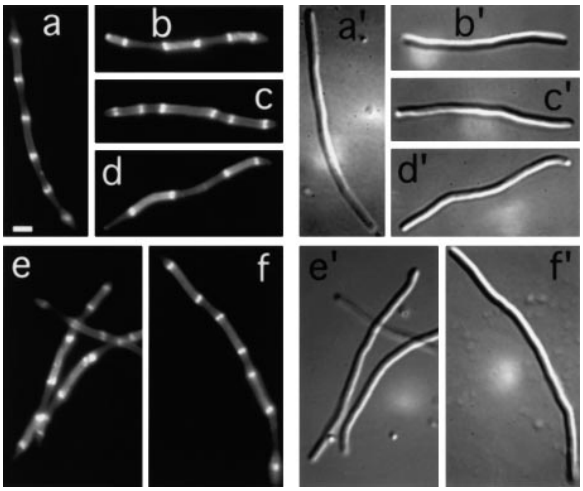

Figure 5. Localization of MinE-Gfp after Induction of SfiA or Depletion of FtsZ

Fluorescence (a–f) and DIC (a′–f′) micrographs showing the presence of multiple MinE-Gfp ring structures in live filaments obtained by induction of SfiA (a and b) or by specific depletion of FtsZ (c–f). For (a) and (b), an overnight culture of strain PB114(λDR144)/pDR123 [Δ*minCDE*(P_{lac}::*sfiA*)/aadA::*minDE-gfp*] was diluted 200-fold in LB with 100 μM (a) or 50 μM (b) IPTG, and cells were immediately observed after growth at 30°C to an optical density (600 nm) of 0.8. For (c)–(f), overnight cultures of PB143/pDB346/pDR112 [*ftsZ*^{0}/$P_{\lambda R}$::*ftsZ*, *cI*857/P_{lac}::*minDE-gfp*] (c and d) and DR102/pDB346/pDR112 [*ftsZ*^{0}, Δ*minCDE*/$P_{\lambda R}$::*ftsZ*, *cI*857/P_{lac}::*minDE-gfp*] (e and f) were diluted 300-fold in LB with 25 μM IPTG. Cells were grown at 42°C until the optical density reached 0.1 and next incubated at 30°C to an optical density between 0.7 and 0.9. The bar represents 2.0 μm.

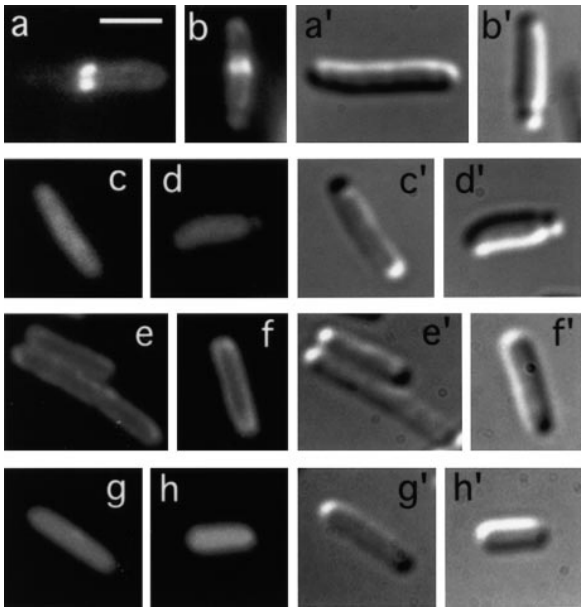

Figure 6. Localization of MinE-Gfp and MinE*-Gfp in the Presence and Absence of MinD

Fluorescence (a–h) and DIC (a′–h′) micrographs of cells from strain PB114 [Δ*minCDE*] carrying plasmid pDR112 [P_{lac}::*minDE-gfp*] (a and b), pDR113 [P_{lac}::*minE-gfp*] (c and d), pDR139 [P_{lac}::*minDE*-gfp*] (e and f), or pDR142 [P_{lac}::*minE*-gfp*] (g and h). Cells were grown in the presence of 25 μM IPTG, and either observed immediately (g and h) or after chemical fixation (a–f). The bar represents 2.0 μm.

which shows cells of DR102/pDB346/pDR112 that were grown in the presence of 25 μM IPTG and shifted from 42°C to 30°C. The failure to divide suggested that the FtsZ level in these filaments had dropped below that required for FtsZ ring formation. This interpretation was supported by quantitative immunoblot analyses showing that the level of FtsZ in these filaments was less than 10% of the normal level at 30°C and was further confirmed by indirect immunostaining of the filaments with FtsZ-specific antibodies, which indicated the complete absence of FtsZ ring structures (data not shown). As shown in Figures 5e and 5f, however, the FtsZ-depleted filaments of DR102/pDB346/pDR112 contained multiple MinE-Gfp rings. Similar results were obtained with a second $FtsZ^{CID}$ strain, PB143/pDB346/pDR112 [*ftsZ*^{0}/$P_{\lambda R}$::*ftsZ*, *cI*857/P_{lac}::*minDE-gfp*], which is identical to DR102/pDB346/pDR112, except that its chromosomal *minB* operon is intact (Figures 5c and 5d). It should be noted that in addition to the examples shown, we also observed many longer filaments with up to more than 30 MinE rings in all three cultures represented in Figure 5. These could not be accurately imaged, however, owing to the instability of the ring structures during microscopy described above. Whereas both the SfiA-induced (Figures 5a and 5b) and $FtsZ^{CID}$ filaments (Figures 5c–5f) contained an average of approximately one ring per 3.0–4.0 μm of cell length, the spacing of rings in the latter appeared less regular than in the former. Perhaps this irregularity is related to readjustment of cell cycle parameters after the temperature shift.

We conclude that assembly of the FtsZ ring is not required for formation of the MinE ring and that the FtsZ protein is unlikely to otherwise play any direct role in this process. In addition, since both PB114(λDR144)/pDR123 and DR102/pDB346/pDR112 lack the *minC* gene, these results also showed that formation of the MinE ring does not require MinC activity.

The MinE Ring Can Be Divorced from Division Sites

A lack of MinC (and/or MinD) in dividing cells gives rise to the classical Min$^-$ phenotype, owing to a frequent misplacement of the division septum near either one of the cell poles (de Boer et al., 1989). To study MinE localization under these conditions, plasmid pDR112 [P_{lac}::*minDE-gfp*] was introduced into strain PB114 [Δ*minCDE*] and cells were analyzed as above. Interestingly, as illustrated in Figures 3f, 3g, 6a, and 6b, MinE-Gfp ring structures were again observed in the great majority (>80%) of live cells (42% after fixation), confirming the notion that MinC is not required for ring assembly. Moreover, despite the high frequency of polar septation events (28 out of 205 cells showed a polar septum), the location of the MinE ring in these cells was similar to that observed in strain PB103/pDR112 in that 98% of the cells with a single ring contained the structure within the central two-fifths portion of the cell (Figure 4a).

As a consequence of the Min$^-$ phenotype, long cells

were relatively abundant in the PB114/pDR112 population, and the fraction of cells with multiple rings was significantly higher (8%) than in strain PB103/pDR112 (<1%). Again, rings appeared to be positioned at regular intervals along the cylindrical part of most of these cells, although we did observe a few long cells with a strong fluorescent signal at one of the poles (data not shown). Polar staining was rare, however, and was only observed in 2 out of 87 randomly chosen cells with clearly defined ring structures.

We conclude that the MinC protein is not required for either the assembly or positioning of the MinE ring. Moreover, the fact that the MinE ring remains located in the central portion of $MinC^-$ cells means that the structure is spatially separated from the polar septation events in these cells.

Involvement of the TS Domain in MinE Ring Formation

Above it was shown that MinE*-Gfp behaved identically to previously described $MinE^{TS-}$ peptides in that it was capable of suppressing MinCD-mediated division inhibition but unable to act in a site-specific manner (Pichoff et al., 1995; Zhao et al., 1995). To determine if this loss in topological specificity correlated with a defect in the proper localization of the protein, we studied the cellular distribution of MinE*-Gfp in strain PB114/pDR139 [Δ*minCDE*/P_{lac}::*minDE*-*gfp*]. Interestingly, MinE*-Gfp failed to accumulate in a ring structure but, rather, appeared to be evenly distributed along the periphery of cells (Figures 6e and 6f). This observation indicates that the TS domain of MinE is not required for an association with the cell envelope per se but is required for the protein to accumulate at midcell.

MinE Ring Formation Is Dependent on MinD

To test whether the MinD protein affected MinE localization, we next studied the distribution of MinE-Gfp in cells lacking MinD. For this experiment, we observed cells of strain PB114/pDR113 [Δ*minCDE*/P_{lac}::*minE-gfp*] after growth in the presence of IPTG. Plasmid pDR113 is identical to pDR112 [P_{lac}::*minDE-gfp*] except that it lacks the *minD* gene. As expected, PB114/pDR113 showed a Min^- phenotype which was similar to that of PB114/pDR112 (Table 1). However, in contrast to PB114/pDR112 (Figures 3f, 3g, 6a, and 6b), PB114/pDR113 failed to show any MinE ring structures at any one of a range of IPTG concentrations (10–250 μM). Instead, cells showed a homogenous fluorescent signal throughout the cell body, indicating that MinE-Gfp was dispersed throughout the cytoplasm (Figures 6c and 6d). These results demonstrated that MinD played a critical role in the localization of MinE-Gfp.

To define the role of MinD in this process further, we next determined the localization of the MinE*-Gfp fusion in cells lacking MinD. As shown in Figure 6, cells of strain PB114/pDR142 [Δ*minCDE*/P_{lac}::*minE*-*gfp*] failed to show the peripheral distribution of MinE*-Gfp that was observed in PB114/pDR139 [Δ*minCDE*/P_{lac}::*minDE*-*gfp*] (e and f). Rather, as was observed in strain PB114/pDR113 (c and d), cells showed an homogenous fluorescence signal (g and h), demonstrating that the apparent association of MinE*-Gfp with the cell envelope was also dependent on the presence of MinD.

Interestingly, the distribution patterns of MinE-Gfp and MinE*-Gfp also appeared to be significantly affected by the manner in which MinD was coexpressed. As discussed above, well-defined ring structures were observed in the vast majority of cells when MinD and MinE-Gfp were coexpressed in *cis* from plasmid pDR112 [P_{lac}::*minDE-gfp*] in either strain PB103 [wt] or PB114 [Δ*minCDE*]. Furthermore, these cells showed a relatively low level of background fluorescence, rendering rings easily discernible and suggesting that most of the MinE-Gfp molecules in the cell were part of this structure. In contrast, the distribution of the fusion was much less defined in strains where *minE-gfp* and *minD* were expressed in *trans*. Thus, although MinE ring structures could also be discerned in normally dividing cells of strain PB114(λDB173)/pDR124 [Δ*minCDE*(P_{lac}::*minCD*)/aadA::*minE-gfp*], they were largely obscured by a significant level of fluorescence, which was homogeneously distributed throughout the cells (Figure 2f). This observation suggests that, although a sufficient amount of MinE-Gfp assembled correctly into a functional ring structure, a significant fraction of the fusion expressed in these cells remained in the cytoplasm. In addition, cells of strain PB103/pDR113 [wt/P_{lac}::*minE-gfp*] also showed a high level of fluorescence in the cytoplasm, and we were unable to discern any specific localization of MinE-Gfp (Table 1) at any one of a range of IPTG concentrations (10–250 μM). It cannot be excluded that a fraction of the MinE-Gfp protein in these cells was associated with a ring structure, however, since the level of dispersed fluorescence may well have precluded this from being visible.

Similarly, the specific localization of the MinE*-Gfp fusion to the cell periphery was most clearly evident when *minD* and *minE*-gfp* were coexpressed in *cis*. Thus, although some preference of MinE*-Gfp for the cell envelope could still be detected in strain PB103/pDR142 [wt/P_{lac}::*minE*-gfp*], this appeared much less pronounced than in cells carrying pDR139 [P_{lac}::*minDE*-*gfp*], (Table 1).

Taken together, these results indicate that MinD is not only required for the localization of MinE, but also that the process is significantly more efficient when the two corresponding genes are expressed in *cis*, rather than in *trans*.

Discussion

Work in recent years has revealed that formation of the division septum in bacteria is mediated by the septal ring, a membrane-associated organelle consisting of the FtsZ ring and associated division proteins. This structure is assembled well before the initiation of cell constriction and remains associated with the leading edge of the invaginating cell wall until division is completed. To date, FtsZ, FtsA, and ZipA have been shown to be part of the septal ring in E. coli, and it is likely that most of the other known division factors are also associated with this structure during some stage of the division cycle (Bi and Lutkenhaus, 1991; Addinall and Lutkenhaus, 1996; Addinall et al., 1996; Ma et al., 1996; Hale and de Boer, 1997).

Table 1. Cellular Location of MinE-Gfp and MinE*-Gfp

Strain	Genotype	Plasmid	Genotype	Division Phenotype	Fluorescence Distribution
PB103	wt	pDR112	P_{lac}::*minDE-gfp*	WT	R
PB103	wt	pDR113	P_{lac}::*minE-gfp*	WT/Min$^-$	C
PB103	wt	pDR139	P_{lac}::*minDE*-gfp*	WT	E
PB103	wt	pDR142	P_{lac}::*minE*-gfp*	WT/Min$^-$	C/E
PB114	Δ*minCDE*	pDR112	P_{lac}::*minDE-gfp*	Min$^-$	R
PB114	Δ*minCDE*	pDR113	P_{lac}::*minE-gfp*	Min$^-$	C
PB114	Δ*minCDE*	pDR139	P_{lac}::*minDE*-gfp*	Min$^-$	E
PB114	Δ*minCDE*	pDR142	P_{lac}::*minE*-gfp*	Min$^-$	C

Cells containing the indicated plasmids were grown in the presence of 25 μM IPTG and inspected by both differential interference contrast and fluorescence microscopy. WT, normal cells and a rare minicell; Min$^-$, normal cells, short filaments, and minicells; WT/Min$^-$, mixed phenotype (cells carrying plasmids pDR113 and pDR142 produced noticeably more minicells than cells carrying pDR112 and pDR139, respectively); R, fluorescent ring at or near the middle of cells; C, cytoplasm, even distribution throughout cell body; E, cell envelope, even distribution along cell periphery; C/E, preference for cell envelope still visible, but also a significant amount of fluorescence in cytoplasm.

Here, a biologically active MinE-Gfp fusion protein was also found to localize early in the division cycle to a ringlike structure at or near the middle of normally dividing cells. Interestingly, however, several lines of evidence imply that MinE is not part of the septal ring organelle but, rather, defines a distinct cell structure. First, unlike FtsZ, ZipA, and FtsA, MinE disappeared from midcell during constriction at this site. This observation indicates that MinE does not actively participate in the constriction process, which is consistent with the fact that MinE is not required for septum formation per se (de Boer et al., 1989). Second, MinE did not localize to the cell poles, but remained in a ring near the middle of minicell producing MinC$^-$ cells, implying that MinE is not merely recruited by septal ring structures but must respond to different positional cues. Third, multiple MinE-Gfp rings were present in filaments that lacked septal rings owing to a block in the assembly of the FtsZ ring, indicating that MinE ring assembly proceeds normally regardless of whether septal rings are formed or not. Further supporting this interpretation, we have observed that MinE rings also continue to be formed in filaments lacking ZipA (data not shown), a recently identified inner-membrane protein that forms a complex with FtsZ at a very early stage of septal ring assembly (Hale and de Boer, 1997).

Combined with the knowledge that MinCD blocks FtsZ ring assembly (Bi and Lutkenhaus, 1993) and that MinE can suppress this block (de Boer et al., 1989; Pichoff et al., 1995; Zhao et al., 1995; Huang et al., 1996), our results support a model in which the normal division cycle of E. coli includes the following order of events: 1) soon after birth, MinE accumulates in a membrane-associated ringlike structure at or near the middle of the long axis of the cell; 2) this results in a localized suppression of MinCD-mediated division inhibition, allowing assembly of the FtsZ ring in proximity of the MinE ring; 3) additional division proteins are recruited to the FtsZ ring, resulting in a mature septal ring organelle; 4) the septal ring initiates constriction and the MinE ring disassembles; 5) constriction is completed, MinE rings assemble at the middle of the two daughter cells, and MinCD prevents the formation of FtsZ rings elsewhere in the cells.

In principle, the location of the MinE ring could be sufficient to identify the correct site of septal ring assembly without further restrictions. As based on the phenotype of minicelling mutants, however, each normal cell appears to contain only three potential division sites (Adler et al., 1967; Teather et al., 1974; de Boer et al., 1989; Lutkenhaus, 1993; Donachie and Begg, 1996; Rothfield and Zhao, 1996). Assuming this interpretation is correct, the MinE ring is not the sole determinant of the site of division but, rather, acts as a selection device to specifically promote usage of the PDS that is present at midcell (Figure 4b).

Our results show that the MinE ring is present in young cells and only appears to disassemble during cell constriction. Combined with the observations that the septal ring is also already present in young cells (Addinall and Lutkenhaus, 1996; Addinall et al., 1996; Ma et al., 1996; Hale and de Boer, 1997), this finding indicates that the two ring structures coexist at midcell during most of the cell cycle. In this regard, it is interesting that the MinE ring was often observed to be located somewhat off-center (Figures 3 and 4a), suggesting that the two ring structures may abut each other rather than being precisely superimposed. The observation that the MinE ring is absent at the division site during constriction suggests that MinCD is incapable of blocking septation once it has initiated, which is consistent with the smooth appearance of filaments after induction of MinCD in the absence of MinE (de Boer et al., 1989).

The identification of the MinE ring as an autonomous division-related cell structure raises many new questions concerning its assembly, composition, and biochemical activities. In this regard, the various roles of the MinD protein in the MinCDE system are particularly intriguing. In previous work, we showed that MinD is not only required for MinC function but also for rendering the MinCD division block sensitive to suppression by MinE (de Boer et al., 1989, 1990, 1991, 1992b). Consistent with those studies, more recent yeast two-hybrid experiments have indicated that MinD binds directly to either MinC or MinE, but not to both at once (Huang et al., 1996). Surprisingly, the current work revealed a third role for MinD in the MinCDE system in that the protein is also clearly required for the proper localization of MinE, highlighting the notion that the MinD protein is not only required for proper functioning of the division inhibitor but also for that of the suppressor of this inhibitor. Thus, in the presence of MinD, MinE-Gfp accumulated into the ring structure, and MinE*-Gfp accumulated (less specifically) at the cell periphery. In the absence of MinD, however, both fluorescent proteins remained

dispersed throughout the cell. Together with the fact that MinD itself is peripherally associated with the cytoplasmic membrane (de Boer et al., 1991), these results suggest a two-stage mechanism for the localization of MinE involving different domains of the MinE peptide.

In the first stage, binding of MinE to MinD results in an association with the membrane. An N-terminal domain of MinE is likely both required and sufficient for this stage since deletion of aa 2–22 abolished its interaction with MinD in the two-hybrid assay (Huang et al., 1996) and since, as shown here, MinE*-Gfp still localized to the membrane in a MinD-dependent fashion. Interestingly, our observations also indicate that efficient localization (and, we suspect, efficient functioning) of MinE requires that *minD* and *minE* be expressed in *cis*. Although it is possible that MinD and MinE associate with the membrane in consecutive order, this phenomenon is more compatible with a model in which newly translated MinD binds the N terminus of nascent MinE and subsequently has to guide the completed peptide toward the membrane.

In the second stage, membrane-associated MinE accumulates at midcell. It is possible that MinD is also involved in this step. However, MinD itself does not appear to accumulate in the ring structure (de Boer et al., 1991; unpublished data), suggesting that MinD and MinE disengage before this step. Regardless, it is clear that the C-terminal TS domain of MinE is required during this stage, as based on the fact that cells lacking this domain show the Min$^-$ phenotype (Pichoff et al., 1995; Zhao et al., 1995) and on our finding that MinE*-Gfp failed to accumulate in the ring structure.

How does MinE find the middle of the cell? Evidently, MinE responds to some topological marker (factor Y in Figure 4b), which uniquely defines midcell and must, therefore, be distinct from the hypothetical factor (factor X in Figure 4b) postulated to mark each PDS. In the simplest model, factor Y is a molecule that binds the TS domain of MinE. Ultimately, however, the positioning of MinE can be expected to be determined by a cellular rather than a molecular parameter. To determine the nature of this parameter remains a major challenge.

Interestingly, the Bacillus subtilis *min* operon lacks a *minE* homolog (Levin et al., 1992; Varley and Stewart, 1992; Lee and Price, 1993), and recent studies have indicated that topological specificity of the MinCD division inhibitor in this organism is at least partly regulated by the product of the unlinked *divIVA* gene (Cha and Stewart, 1997; Edwards and Errington, 1997). The primary structure of DivIVA shows no significant similarity to MinE, however, and genetic analyses suggest that the mechanism of DivIVA action is fundamentally different from that of MinE (Cha and Stewart, 1997; Edwards and Errington, 1997). This suggestion is supported by the contrasts between this and concurrent localization studies in which a DivIVA-Gfp fusion was found to localize to both the division septa and cell poles of Bacillus subtilis (Edwards and Errington, 1997). In addition, DivIVA localization was shown to be independent of MinD but strictly dependent on FtsZ (D. Edwards and J. Errington, personal communication). These results indicate that DivIVA is recruited to division sites only after the FtsZ ring has already formed and that it remains at the cell poles after constriction is completed, supporting the proposal that DivIVA plays a role in attracting MinCD to its site of action (Cha and Stewart, 1997; Edwards and Errington, 1997). Whether the topological specificity of MinCD in B. subtilis is, in addition, also determined by a MinE-like ring structure remains to be seen.

Finally, throughout our studies with the MinE-Gfp protein, we noticed an interesting phenomenon that was most easily seen in filamentous cells such as those shown in Figure 5. Although most of the fluorescent protein in these filaments accumulated into well-defined ring structures, some fluorescence was often also seen in the area between a cell pole and the nearest ring, or between two neighboring rings. This extraannular signal, furthermore, was strongest at the cell periphery (best seen in Figure 5c), suggesting it was primarily associated with the cell envelope. Curiously, however, this signal was not evenly distributed over the cell envelope of the filaments but, rather, produced an alternating zebralike pattern such that each brightly fluorescent ring structure was always flanked by one nonfluorescent and one weakly fluorescent cell segment (Figures 5b–5e). Although this nonrandom pattern was most obvious in filaments, a similar phenomenon was also observed in Sep$^+$ cells where fluorescence that was not associated with the ring was often noticeably stronger on one side of the ring than on the other (e.g., the most left-hand cells in Figures 3a and 3g, and 6a). The presence of MinE molecules outside of the ring structure is by itself not surprising. The ring can be expected to be a dynamic structure, and the extraannular MinE-Gfp may have represented normal intermediates in the assembly or disassembly of the structure. Alternatively, ring structures may have been saturated with MinE-Gfp, causing some of the protein to spill over to other parts of the cell envelope. Whatever the purpose and/or cause of the extraannular MinE-Gfp, however, its asymmetric distribution is remarkable and implies that the protein can somehow discriminate between the two cell halves on either side of the MinE ring. This raises the possibility that the MinE ring is not only instrumental in selection of the proper division site but may also be involved in maintaining or establishing polarity in the E. coli cell.

Experimental Procedures

Strains, Plasmids, and Phages

Strains PB103 [*dadR*$^-$, *trpE*$^-$, *trpA*$^-$, *tna*$^-$], PB114 [PB103, Δ*minCDE*::*aph*], DX1 [PB103, Δ*minCDE*::*aph*, *recA*::Tn10] (de Boer et al., 1991), and WX7/pCX41 [PB103, *ftsZ*^{0}, *leu*::Tn10/*repA*^{ts}, *ftsZ*] (Wang et al., 1991) have been described. A P1 lysate was prepared on DX1 and first used to transduce WX7/pCX41 to *leu*$^+$ yielding PB142/pCX41[PB103, *ftsZ*^{0}/*repA*^{ts}, *ftsZ*]. The same lysate was next used to transduce PB142/pCX41 to *recA*::Tn10, yielding PB143/pCX41, or first to Δ*minCDE*::*aph* and then to *recA*::Tn10, yielding DR102/pCX41. Strains PB143/pDB346/pDR112 [PB103, *ftsZ*^{0}, *recA*::Tn10/$P_{\lambda R}$::*ftsZ*, *cI*857/P_{lac}::*minDE-gfp*] and DR102/pDB346/pDR112 [PB103, Δ*minCDE*::*aph*, *ftsZ*^{0}, *recA*::Tn10/$P_{\lambda R}$::*ftsZ*, *cI*857/P_{lac}::*minDE-gfp*] were subsequently obtained by substitution of plasmid pCX41 with pDB346, followed by transformation with pDR112.

Plasmids pXX147 (Hiraga et al., 1989), pMLB1115 and pDB156 (de Boer et al., 1989), pDB183 (de Boer et al., 1990), and pZC100 (Zhao et al., 1995) have been described previously.

Plasmid pDB346 [$P_{\lambda R}$::*ftsZ*, *cI*857] was obtained by first inserting

a fragment containing the λ*R* promotor and *cI*857 allele of pXX147 into pZC100, followed by insertion of a promotorless *ftsZ* fragment into the resulting plasmid (pDB344). The *ftsZ* gene of pDB346 is transcribed in the orientation opposite that of the spectinomycin resistance gene (*aadA*). Relevant features of the remaining plasmids are illustrated in Figure 1 and discussed in the text.

Phage λDB173 has been described (de Boer et al., 1989). Phage λDR144 [P_{lac}::*sfiA*] is a derivative of λNT5 (de Boer et al., 1989) and contains the *sfiA* gene downstream the *lac* promotor.

Microscopy

Unless noted otherwise, overnight cultures were diluted 133-fold in fresh LB medium with the appropriate supplements and grown at 30°C until the optical density (600 nm) reached 0.8–1.2. Cells were examined either immediately (live cells) or after chemical fixation. To fix cells, a mixture of glutaraldehyde (to 0.2%) and formaldehyde (to 6.0%) was immediately added to a sample of the culture. Cells were incubated at room temperature for 45 min, collected by centrifugation, resuspended in one-tenth the volume 0.9% saline, and kept at 4°C until microscopic examination. Microscopy and image handling were done as described (Hale and de Boer, 1997). Cell parameters were measured using NIH Image (1.61).

Acknowledgments

We thank Cynthia Hale, Dinesh Rao, and Gregory Matera for technical assistance and advice; Brendan Cormack and Sota Hiraga for the gift of plasmids; Timothy Nilsen, Robert Hogg, and Cynthia Hale for critical comments on the manuscript; and David Edwards and Jeffery Errington for allowing use of their unpublished data. This work was supported by an NSF young investigator award (MCB94-58197) and generous donations from the Elizabeth M. and William C. Treuhaft Fund, the Frank K. Griesinger Trust, Mrs. Arline H. Garvin, Mr. James S. Blank, Mr. Charles E. Spahr, Dr. Alfred M. Taylor, and Dr. Theodore J. Castele. D. M. R. was supported by an NRSA Institutional Training Grant (T32GM08056) from the NIH.

Received August 22, 1997; revised October 15, 1997.

References

Addinall, S.G., and Lutkenhaus, J. (1996). FtsA is localized to the septum in an FtsZ-dependent manner. J. Bacteriol. *178*, 7167–7172.

Addinall, S.G., Bi, E., and Lutkenhaus, J. (1996). FtsZ ring formation in *fts* mutants. J. Bacteriol. *178*, 3877–3884.

Adler, H.I., Fisher, W.D., Cohen, A., and Hardigree, A.A. (1967). Miniature Escherichia coli cells deficient in DNA. Proc. Natl. Acad. Sci. USA. *57*, 321–326.

Baumann, P., and Jackson, S.P. (1996). An archaebacterial homologue of the essential eubacterial cell division protein FtsZ. Proc. Natl. Acad. Sci. USA *93*, 6726–6730.

Bi, E., and Lutkenhaus, J. (1990). Interaction between the *min* locus and *ftsZ*. J. Bacteriol. *172*, 5610–5616.

Bi, E., and Lutkenhaus, J. (1991). FtsZ ring structure associated with division in Escherichia coli. Nature *354*, 161–164.

Bi, E., and Lutkenhaus, J. (1993). Cell division inhibitors, SulA and MinCD, prevent formation of the FtsZ ring. J. Bacteriol. *175*, 1118–1125.

Cha, J.-H., and Stewart, G.-C. (1997). The divIVA minicell locus of Bacillus subtilis. J. Bacteriol. *179*, 1671–1683.

Cormack, B.P., Valdivia, R.H., and Falkow, S. (1996). FACS-optimized mutants of the green fluorescent protein (GFP). Gene *173*, 33–38.

de Boer, P.A.J., Crossley, R.E., and Rothfield, L.I. (1988). Isolation and properties of *minB*, a complex genetic locus involved in correct placement of the division site in Escherichia coli. J. Bacteriol. *170*, 2106–2112.

de Boer, P.A.J., Crossley, R.E., and Rothfield, L.I. (1989). A division inhibitor and a topological specificity factor coded for by the minicell locus determine proper placement of the division septum in E. coli. Cell *56*, 641–649.

de Boer, P.A.J., Crossley, R.E., and Rothfield, L.I. (1990). Central role for the Escherichia coli *minC* gene product in two different cell division-inhibition systems. Proc. Natl. Acad. Sci. USA *87*, 1129–1133.

de Boer, P.A.J., Crossley, R.E., Hand, A.R., and Rothfield, L.I. (1991). The MinD protein is a membrane ATPase required for the correct placement of the Escherichia coli division site. EMBO J. *10*, 4371–4380.

de Boer, P., Crossley, R., and Rothfield, L. (1992a). The essential bacterial cell-division protein FtsZ is a GTPase. Nature *359*, 254–256.

de Boer, P.A.J., Crossley, R.E., and Rothfield, L.I. (1992b). Roles of MinC and MinD in the site-specific septation block mediated by the MinCDE system of Escherichia coli. J. Bacteriol. *174*, 63–70.

Donachie, W.D., and Begg, K.J. (1996). Division potential in Escherichia coli. J. Bacteriol. *178*, 5971–5976.

Edwards, D.H., and Errington, J. (1997). The Bacillus subtilis DivIVA protein targets to the division septum and controls the site specificity of cell division. Molec. Microbiol. *24*, 905–915.

Erickson, H.P., Taylor, D.W., Taylor, K.A., and Bramhill, D. (1996). Bacterial cell division protein FtsZ assembles into protofilament sheets and minirings, structural homologs of tubulin polymers. Proc. Natl. Acad. Sci. USA *93*, 519–523.

Hale, C.A., and de Boer, P.A.J. (1997). Direct binding of FtsZ to ZipA, an essential component of the septal ring structure that mediates cell division in E. coli. Cell *88*, 175–185.

Higashitani, A., Higashitani, N., and Horiuchi, K. (1995). A cell division inhibitor SulA of Escherichia coli directly interacts with FtsZ through GTP hydrolysis. Biochem. Biophys. Res. Comm. *209*, 198–204.

Hiraga, S., Niki, H., Ogura, T., Ichinose, C., Mori, H., Ezaki, B., and Jaffe, A. (1989). Chromosome partitioning in Escherichia coli: novel mutants producing anucleate cells. J. Bacteriol. *171*, 1496–1505.

Huang, J., Cao, C., and Lutkenhaus, J. (1996). Interaction between FtsZ and inhibitors of cell division. J. Bacteriol. *178*, 5080–5085.

Lee, S., and Price, C.W. (1993). The minCD locus of Bacillus subtilis lacks the minE determinant that provides topological specificity to cell division. Mol. Microbiol. *7*, 601–610.

Levin, P., Margolis, P.S., Setlow, P., Losick, R., and Sun, D. (1992). Identification of Bacillus subtilis genes for septum placement and shape determination. J. Bacteriol. *174*, 6717–6728.

Lutkenhaus, J. (1993). FtsZ ring in bacterial cytokinesis. Molec. Microbiol. *9*, 403–409.

Lutkenhaus, J., and Mukherjee, A. (1996). Cell division. In Escherichia coli and Salmonella., F.C. Neidhardt, ed. (Washington, D.C.: ASM Press), pp. 1615–1626.

Ma, X., Ehrhardt, D.W., and Margolin, W. (1996). Colocalization of cell division proteins FtsZ and FtsA to cytoskeletal structures in living Escherichia coli cells by using green fluorescent protein. Proc. Natl. Acad. Sci. *93*, 12998–13003.

Margolin, W., Wang, R., and Kumar, M. (1996). Isolation of an *ftsZ* homolog from the archaebacterium Halobacterium salinarium: implications for the evolution of FtsZ and Tubulin. J. Bacteriol. *178*, 1320–1327.

Mukherjee, A., Dai, K., and Lutkenhaus, J. (1993). Escherichia coli cell division protein FtsZ is a guanine nucleotide binding protein. Proc. Natl. Acad. Sci. USA *90*, 1053–1057.

Mukherjee, A., and Lutkenhaus, L. (1994). Guanine nucleotide-dependent assembly of FtsZ into filaments. J. Bacteriol. *176* , 2754–2758.

Pichoff, S., Vollrath, B., Touriol, C., and Bouché, J.-P. (1995). Deletion analysis of gene *minE* which encodes the topological specificity factor of cell division in Escherichia coli. Molec. Microbiol. *18*, 321–329.

RayChaudhuri, D., and Park, J.T. (1992). Escherichia coli cell-division gene *ftsZ* encodes a novel GTP-binding protein. Nature *359*, 251–254.

Rothfield, L.I., and Justice, S.S. (1997). Bacterial cell division: the cycle of the ring. Cell *88*, 581–584.

Rothfield, L.I., and Zhao, C.-R. (1996). How do bacteria decide where to divide? Cell *84*, 183–186.

Teather, R.M., Collins, J.F., and Donachie, W.D. (1974). Quantal behavior of a diffusible factor which initiates septum formation at potential division sites in Escherichia coli. J. Bacteriol *118*, 407–413.

Varley, A.W., and Stewart, G.C. (1992). The *divIVB* region of the Bacillus subtilis chromosome encodes homologs of Escherichia coli septum placement (MinCD) and cell shape (MreBCD) determinants. J. Bacteriol. *174*, 6729–6742.

Wang, X., de Boer, P.A.J., and Rothfield, L.I. (1991). A factor that positively regulates cell division by activating transcription of the major cluster of essential cell division genes of Escherichia coli. EMBO J. *10*, 3363–3372.

Ward, J.E., and Lutkenhaus, J. (1985). Overproduction of FtsZ induces minicell formation in E. coli. Cell *42*, 941–949.

Zhao, C.-R., de Boer, P.A.J., and Rothfield, L.I. (1995). Proper placement of the Escherichia coli division site requires two functions that are associated with different domains of the MinE protein. Proc. Natl. Acad. Sci. USA *92*, 4314–4317.